ACS Chemical Neuroscience

Letter

pubs.acs.org/chemneuro

Biological Activity of *sym*-Triazines with Acetylcholine-like Substitutions as Multitarget Modulators of Alzheimer's Disease

Anthony J. Veloso,[†] Ari M. Chow,[‡] Devjani Dhar,[†] Derek W. F. Tang,[‡] Hashwin V.S. Ganesh,[‡] Svetlana Mikhaylichenko,[†] Ian R. Brown,[‡] and Kagan Kerman*[,†,‡]

[†]Department of Physical and Environmental Sciences and [‡]Centre for the Neurobiology of Stress, Department of Biological Sciences, University of Toronto Scarborough, 1265 Military Trail, Toronto, ON M1C 1A4, Canada

ABSTRACT: The bioactivities of two novel compounds (TAE-1 and TAE-2) that contain a *sym*-triazine scaffold with acetylcholine-like substitutions are examined as promising candidate agents against Alzheimer's disease. Inhibition of amyloid-β fibril formation in the presence of Aβ_{1-42}, evaluated by Thioflavin T fluorescence, demonstrated comparable or improved activity to a previously reported pentapeptide-based fibrillogenesis inhibitor, iAβ5p. Destabilization of Aβ_{1-42} assemblies by TAE-1 and TAE-2 was confirmed by scanning electron microscopy imaging. *sym*-Triazine inhibition of acetylcholinesterase (AChE) activity was observed in cytosol extracted from differentiated human SH-SY5Y neuronal cells and also using human erythrocyte AChE. The *sym*-triazine derivatives were well tolerated by these cells and promoted beneficial effects on human neurons, upregulating expression of synaptophysin, a synaptic marker protein, and MAP2, a neuronal differentiation marker.

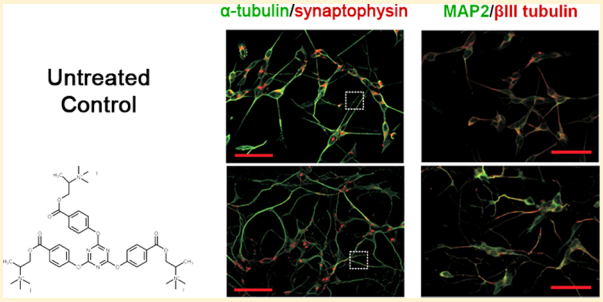

KEYWORDS: *Amyloid-beta, sym-triazines, acetylcholinesterase, multitarget modulator, Alzheimer's disease, human SH-SY5Y neuronal cells*

Alzheimer's disease (AD) is a progressive neurodegenerative disorder characterized by the cerebral accumulation of insoluble aggregates of amyloid-β peptides (Aβ).[1] While the precise mechanisms governing neuronal loss remains ambiguous, toxicity resulting from Aβ-activated pathways is evident.[2,3] Consequently, efforts to mitigate neurodegeneration have emphasized the removal of Aβ aggregates. Oligomerization of natively soluble Aβ monomers is fundamentally dependent on the self-assembly of highly ordered cross β-sheet quaternary structures, which stack by an in-register and antiparallel arrangement.[4] These prefibril oligomeric species have been identified as the more relevant structural derivatives in Aβ-induced toxicity.[5]

To this effect, a variety of small molecule inhibitors have been reported to impede hydrophobic association and fibrillogenesis of Aβ by disrupting β-sheet $\pi-\pi$ stacking.[6,7] Alternatively, current FDA-approved drug therapy strategies attempt to ameliorate the significant pathological reduction of the neurotransmitter acetylcholine (ACh)[8] by modulating the hydrolytic activity of acetylcholinesterase (AChE) with small-molecule inhibitors.[9,10] However, disease progression in AD is multifactorial in nature, and hence, targeted inhibition of a single disease pathology is compensated by concurrent deleterious pathways.[11,12] Combination therapies, which implement numerous drug entities to target multiple pathologies simultaneously, have thus emerged as strong candidates for the development of effective disease-modifying strategies.[12] In view of the above, complications associated with the administration of multiple single-target drug entities such as conflicting bioavailabilities, pharmacokinetics, and metabolism may be circumvented through the implementation of multitarget therapies. Such strategies can further serve to minimize cross-reactivity and simplify therapeutic regimens while facilitating streamlined clinical development.[13] Interestingly, individual multitarget treatments have in some cases demonstrated improved therapeutic properties over their single-target counterparts.[14]

We describe the biological activity of two novel *sym*-triazine derivatives containing ACh-like substitutions (TAE-1, TAE-2) for modulation of Aβ_{1-42} aggregation and AChE hydrolytic activity (Figure 1). We have recently detailed the synthesis of a small library of sym-triazines with various modifications possessing multitarget activity.[15] Considering the high activities of TAE-1 and TAE-2 (also designated 3f and 3g),[15] the development of viable drug candidates necessitates an evaluation of their biological activity on differentiated human SH-SY5Y neuronal cells.

RESULTS AND DISCUSSION

In AD affected individuals, Aβ is present in two major isoforms, Aβ_{1-40} and Aβ_{1-42}. Aβ_{1-42} contains two additional hydrophobic amino acids (Ile, Ala) at the C-terminus that stimulate a faster

Received: January 24, 2013
Accepted: March 10, 2013
Published: March 11, 2013

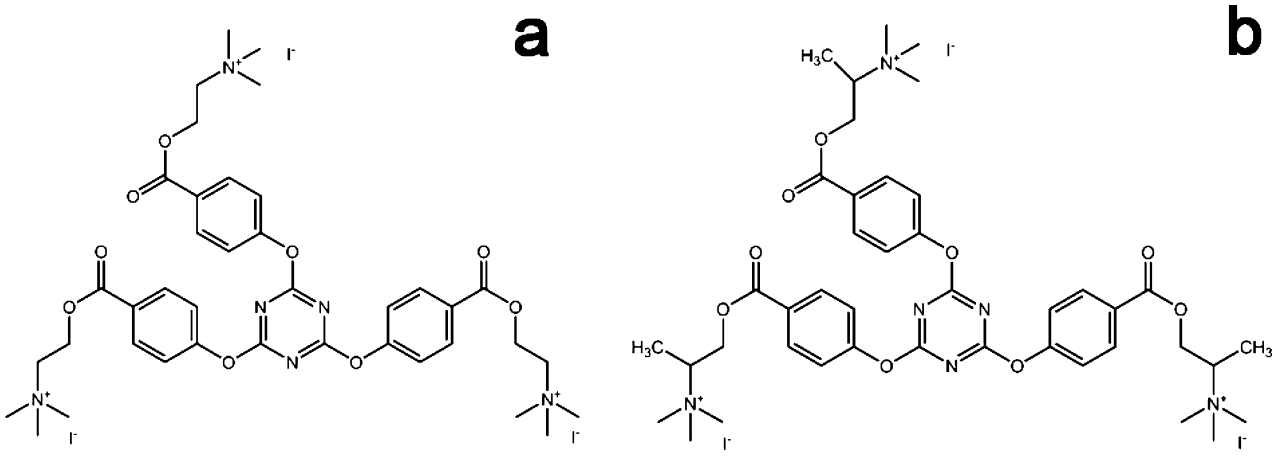

Figure 1. Chemical structures of (a) TAE-1 and (b) TAE-2.

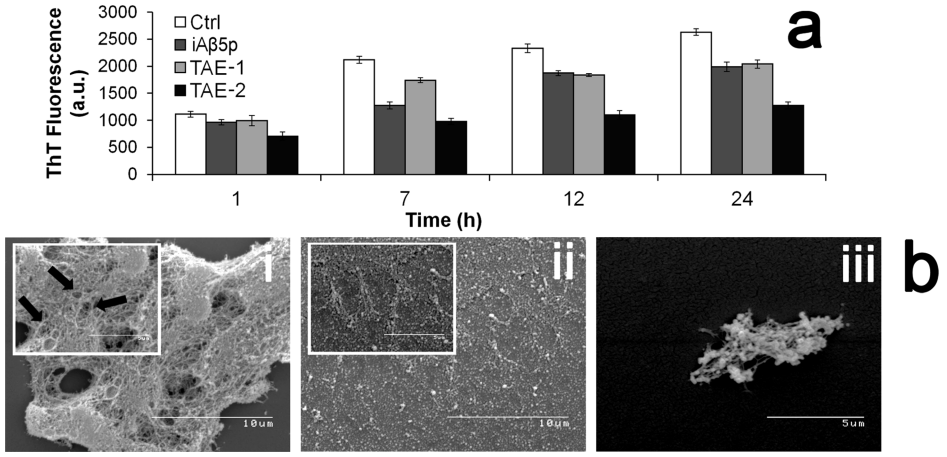

Figure 2. Effect of TAE-1 and TAE-2 on Aβ_{1-42} fibril formation. (a) ThT fluorescence (λ_{EX} 440 nm, λ_{EX} 485 nm), in which Aβ_{1-42} (10 μM) was incubated at 37 ± 1 °C and shaking at 300 rpm for up to 24 h with 20 μM iAβ5p, TAE-1, or TAE-2, $n \geq 3$; Ctrl denotes Aβ_{1-42} (10 μM) sample in the absence of modulators. (b) Scanning electron microscopy for (i) 50 μM Aβ_{1-42}, (ii) 50 μM Aβ_{1-42} with 50 μM TAE-1, and (iii) 50 μM Aβ_{1-42} with 50 μM TAE-2, incubated at 37 ± 1 °C for 2 weeks. All samples described above were prepared in 50 mM PBS with 100 mM NaCl adjusted to pH 7.4. Black arrows indicate areas of fibril formation.

rate of aggregation, forms insoluble deposits prior to Aβ_{1-40}, and is the predominant amyloid species present within neuritic plaques. We previously characterized the effect of TAE-1 and TAE-2 on modulation of Aβ_{1-40} aggregation,[15] and herein study their effects on Aβ_{1-42}. Analysis of TAE-1 and TAE-2-modulated Aβ_{1-42} fibril growth was determined by kinetic studies using Thioflavin T (ThT) fluorescence measured up to 24 h. The pentapeptide-based fibrillogenesis inhibitor, iAβ5p (Ac-LPFFD-NH_2), served as a comparison for activity of the newly synthesized *sym*-triazines. Figure 2a depicts a decrease in ThT fluorescence intensity at each time interval resulting from the coincubation of Aβ_{1-42} (10 μM) with TAE-1, TAE-2 or iAβ5p (20 μM). Fluorescence studies indicated that *sym*-triazine-based aggregation modulators demonstrated equal or greater fibril inhibition relative to previously reported inhibitor, iAβ5p, for time periods measured after 7 h. Specifically, at 24 h, both TAE-1 and iAβ5p exhibited fibril inhibition corresponding to 24.9% and 22.3%, respectively, measured by the ratio of fluorescence to the uninhibited control. At an equivalent concentration, TAE-2 displayed an even greater reduction of 52.6% β-sheet inhibition. The improved activity of TAE-2 could be attributed to the incorporation of additional hydrophobic and sterically disruptive methyl functional units on ACh-like branches.

It has been noted that many aggregation-modulating agents that demonstrate a profound reduction to Aβ-induced cytoxicity simultaneously alter the structural morphology of fibrils.[16−18] Scanning electron microscopy (SEM) studies demonstrated that a control sample of native Aβ_{1-42} (Figure 2b_i) clearly exhibits an intertwined, meshlike network of fibrillar strands with an approximate width of 10 nm and length greater than 1 μm. Black arrows indicate areas of fibril formation. However, in the presence of the *sym*-triazine inhibitor TAE-1 (Figure 2b_{ii}), truncation of fibrils was evident, as accumulations of smaller spherical clusters were observed. It is suggested that the intercalation of Aβ_{1-42} with TAE-1 facilitated deviation from classical nucleation-dependent fibril formation. In addition, *sym*-triazine-modulated Aβ_{1-42} samples incubated in the presence of TAE-2 (Figure 2b_{iii}) showed decreased aggregation with reduced fibrillation. It was concluded that both inhibitors were effective in decreasing fibril formation, with TAE-2 exhibiting the most pronounced effect, concurrent with ThT fluorescence results. Thus, SEM studies demonstrated the capacity of *sym*-triazine derivatives to influence large-scale fibril formation.

dx.doi.org/10.1021/cn400028w | *ACS Chem. Neurosci.* 2013, 4, 924−929

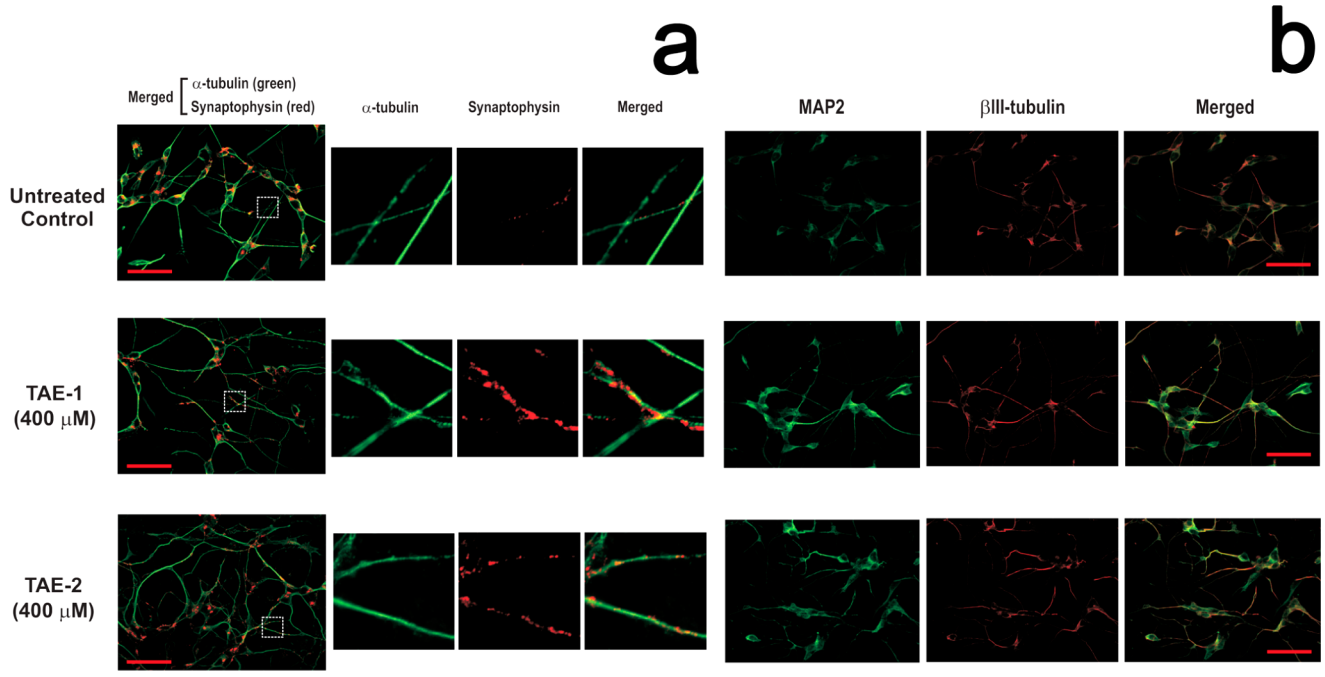

Figure 3. Treatment of differentiated human SH-SY5Y neuronal cells with TAE-1 and TAE-2. (a) Effect on neuronal cellular processes and synaptic marker protein (synaptophysin, red). Neuronal cells highlighted with the cytoskeleton marker protein, α-tubulin (green). Boxed areas shown at higher magnification reveal increased synaptic marker protein along neuronal processes following TAE-1 and TAE-2. (b) Effect of TAE-1 and TAE-2 on the expression of MAP2 (green), a neuronal differentiation marker. βIII-tubulin (red), a neuronal cytoskeleton marker, was employed as a counterstain for neuronal morphology. Neuronal cells treated with TAE-1 and TAE-2 for 24 h in (a) and (b). Images obtained using an AxioCam HRm camera with ApoTome module on an AxioVert 200 M microscope (Carl Zeiss) with a 40× oil objective. Scale bar = 50 μm.

We next examined the effects of TAE-1 and TAE-2 on differentiated human SH-SY5Y neuronal cells grown in tissue culture. As shown in Figure 3a, stimulation of neuronal cellular process length and branching was noted. In addition, increased synaptophysin (a synaptic marker protein) was apparent along varicosities of neuronal cellular processes (high magnification of boxed areas), suggesting that TAE-1 and TAE-2 stimulate synapse formation.[19,20] Increased expression of MAP2 was also observed, suggesting that TAE-1 and TAE-2 promote the differentiation of human neurons (Figure 3b). MAP2 is a marker of neuronal cell differentiation that plays important roles in the growth of neuronal cellular processes.[21−23] βIII-tubulin, a neuronal marker, was used as a counter-stain for neuronal morphology.

Targeted AChE inhibition was evaluated by electrochemical quantification of the enzymatic product, thiocholine (TCh), on unmodified gold screen-printed electrodes (0.3 V vs Ag/AgCl).[24,25] At increasing concentrations of TAE-1 or TAE-2, there was a corresponding decrease in the AChE activity thereby reducing the amount of oxidizable TCh present in solution (Figure 4). The IC_{50} values of 0.465 and 3.931 μM for TAE-1 and TAE-2, respectively, were derived from nonlinear regression of inhibition plots calculated by baseline-corrected peak currents (bar graph insets in Figure 4). We have previously noted that the presence of methyl substituents on TAE-2 resulted in enhanced modulation of Aβ aggregation.[15] We suggested that these same methyl substituents also reduced structural similarities of the aminoester arms to the native AChE substrate, resulting in decreased enzyme binding affinity and weaker inhibition compared to TAE-1.

AChE inhibition studies were conducted using cytosol extracts from differentiated human neuronal cells, which endogenously express AChE.[26] Human neuronal cells were prepared following a previously reported procedure.[26] Analysis of AChE inhibition in neuronal extracts provides a good model for predicting future in vivo applications. AChE activity was determined by Ellman's colorimetric assay (Figure 5).[27,28] Cells were incubated for 24 h with either TAE-1 or TAE-2 at 400 μM, the highest viable concentration tested in our cellular viability studies.[15] Donepezil (Aricept) treatment was used as a positive control for AChE inhibition and is the commonly prescribed AChE inhibitor available for clinical use.[29] Donepezil was applied at a maximum concentration of 10 μM, as previously noted as an effective concentration for inhibition while higher concentrations resulted in reduced viability of differentiated human neuronal cells.[30] It was promising that both TAE-1 and TAE-2 demonstrated effective inhibition of AChE activity, showing a significantly greater inhibition (84.4%, 64.7%, respectively) relative to Donepezil (15.4%) (Figure 5a). Comparable values (86.9%, 41.6%, 17.1%) were also observed for measurements performed using purified human erythrocyte AChE (Figure 5b). The improved inhibition of AChE activity by TAE-1 relative to TAE-2 as measured by Ellman's method was consistent with the electrochemical assay. These results correlate with the observation that TAE-1 has a more prominent effect in inducing neuronal differentiation.

The present study extends our previous work on *sym*-triazine-based multitarget modulators of AD and explores the biological activity of TAE-1 and TAE-2 on human neuronal systems. The new studies indicate that exposure of differentiated human neuronal cells to TAE-1 and TAE-2 upregulates neuronal differentiation as evident by increases in neurite extension, synaptophysin positive varicosities and the neuronal differentiation marker MAP2. These findings indicate that *sym*-triazine derivatives are promising AD therapies, given their capacity to target pathologies of the disease such as Aβ

dx.doi.org/10.1021/cn400028w | *ACS Chem. Neurosci.* 2013, 4, 924−929

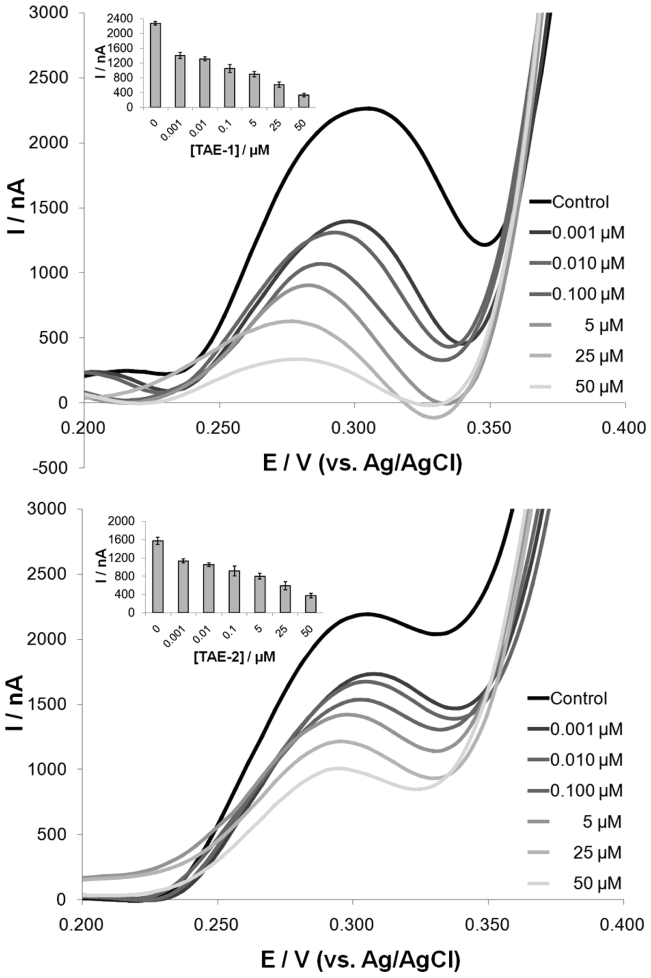

Figure 4. Targeting AChE activity by TAE-1 and TAE-2. Differential pulse voltammetry (DPV) was applied from −0.1 to 0.9 V (vs Ag/AgCl). The voltammograms depict the oxidation of TCh measured at 0.3 V. TCh was produced from the hydrolytic degradation of 550 μM ATCh by 0.1875 U/mL purified human erythrocyte AChE following 10 min of incubation at room temperature. Measurements were conducted on Au screen-printed electrodes in 50 mM PBS, 100 mM NaCl adjusted to pH 7.4. Prior to the addition of ATCh substrate, AChE was preincubated for 30 min with 0.001, 0.010, 0.100, 5, 25, and 50 μM of (a) TAE-1 and (b) TAE-2 and compared to the uninhibited enzyme. The insets show the baseline-corrected peak currents of TCh oxidation at 0.3 V. Error bars denote a standard deviation, $n \geq 3$. Parameters for DPV measurements were adjusted to a 50 mV modulation amplitude, 5 mV step potential, 50 ms modulation time and 10 s equilibration time.

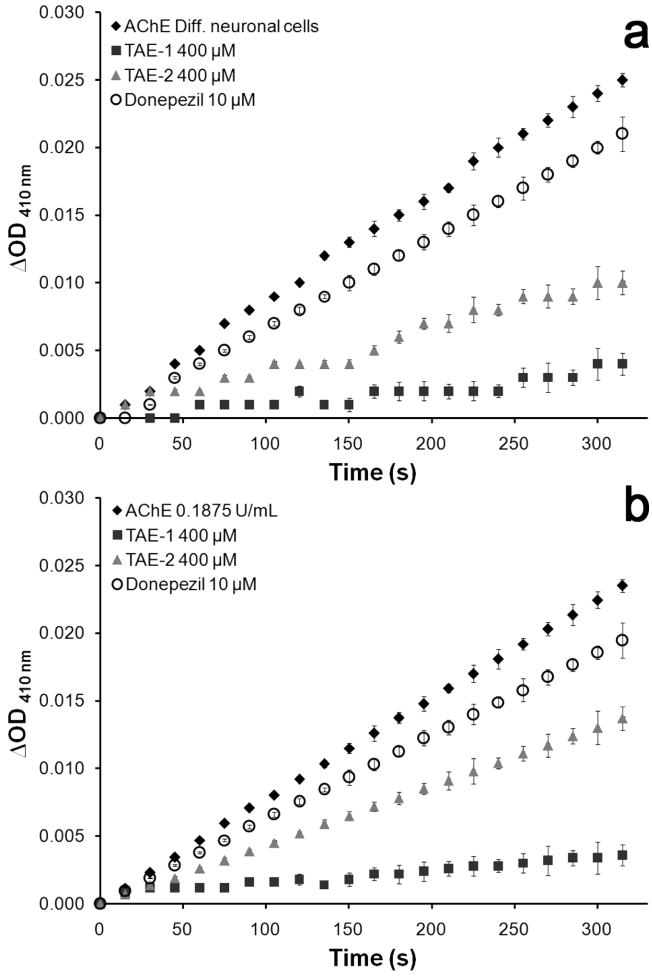

Figure 5. Effect of TAE-1 and TAE-2 on suppressing AChE activity. (a) Cytosol extracted from differentiated human SH-SY5Y neuronal cells and (b) purified human erythrocyte AChE, measured by DTNB colorimetric assay at 410 nm. Cells were incubated in the presence of TAE-1, TAE-2, and Donepezil for 24 h prior to harvesting and preparation of cell extracts. Enzyme reaction was initiated by the simultaneous addition of DTNB (340 μM) and ATCh (550 μM). Absorbance was measured at 410 nm periodically (every 15 s) over an interval of 315. Error bars denote a standard deviation, $n \geq 3$. The rates of initial enzyme activity were derived from the slope of the absorbance−time curves. Measurements were conducted in 50 mM PBS, 100 mM NaCl adjusted to pH 7.4.

aggregation and AChE activity, and in addition to stimulate neuronal differentiation.

In view of the inherent multifactorial nature of AD, multitarget inhibitors have been proposed as viable candidates for the development of effective disease-modifying drug therapies.[12] In this report, we demonstrate the biological activity of two novel molecules to counter AD using *sym*-triazine derivatives as a scaffold for the disruption of both Aβ fibril formation and AChE hydrolytic activity. TAE-1 and TAE-2 are shown to modulate Aβ_{1-42} aggregation. In addition, AChE inhibition by TAE-1 and TAE-2 was evaluated in relevant human biological systems using AChE in cytosol extracts of differentiated human SH-SY5Y neuronal cells and purified human erythrocyte AChE. In complex neurodegenerative diseases such as AD, one has to think beyond the traditional "one molecule, one target" approach. Our design for *sym*-triazines with ACh-like substitutions has generated hybrid molecules that possess multiple beneficial biological activities as potentially disease modifying agents.

METHODS

Chemicals and Reagents. Human amyloid-β peptide 1−42 Gln11 (Aβ_{1-42}; trifluoroacetate salt) ⟨H-Asp-Ala-Glu-Phe-Arg-His-Asp-Ser-Gly-Tyr-Gln-Val-His-His-Gln-Lys-Leu-Val-Phe-Phe-Ala-Glu-Asp-Val-Gly-Ser-Asn-Lys-Gly-Ala-Ile-Ile-Gly-Leu-Met-Val-Gly-Gly-Val-Val-Ile-Ala-OH⟩ was obtained from EMD-Biosciences (Gibbstown, NJ). Dimethyl sulfoxide (DMSO; 99.99%), 1,1,1,3,3,3-hexafluoro-2-propanol (HFIP, 99.0%), Thioflavin T (4-(3,6-dimethyl-1,3-benzothiazol-3-ium-2-yl)-*N*,*N*-dimethylaniline chloride; ∼75%), 5,5′-dithiobis(2-nitrobenzoic acid) (DTNB, >98%), acetylthiocholine iodide (ATCh, >98%), purified human erythrocyte acetylcholinesterase (AChE), sodium phosphate monobasic (NaH_2PO_4; 99.0%), and

dx.doi.org/10.1021/cn400028w | ACS Chem. Neurosci. 2013, 4, 924−929

sodium phosphate dibasic (Na_2HPO_4; 99.0%) were purchased from Sigma-Aldrich (Oakville, ON). All samples were of analytical grade and prepared in phosphate buffer saline (50 mM, PBS), sodium chloride (NaCl, 100 mM) at pH 7.4 using 18.2 MΩ analytical grade water obtained from a Cascada LS water purification system (Pall Co., Mississauga, ON).

Thioflavin T Kinetic Analysis of Aβ Aggregation. ThT stock (10 mM) was prepared in 18.2 MΩ water and stored at 4 ± 1 °C. TAE-1 (1.77 mM) and TAE-2 (1.41 mM) stock solutions were prepared directly into 50 mM PBS, pH 7.4, 100 mM NaCl and stored at 4 ± 1 °C. iAβ5p (Ac-LPFFD-NH_2) and $A\beta_{1-42}$ (553.7 μM) were prepared in dimethyl sulfoxide (DMSO) and stored at −20 ± 1 °C. Sample solutions were equilibrated to RT prior to measurement and diluted to the appropriate concentrations with 50 mM PBS, pH 7.4. Each 200 μL sample was prepared into black optilux fluorescence 96-well plates (BD Biosciences, Mississauga, Canada), containing ThT (10 μM), $A\beta_{1-42}$ (10 μM), and inhibitor (20 μM). Spontaneous aggregation of $A\beta_{1-42}$ samples was induced by incubation at 37 ± 1 °C with shaking at 300 rpm. Fluorescence (λ_{EX} 440 nm, λ_{EM} 485 nm) was measured at various time intervals over 24 h using a Synergy HT Multimode Microplate reader from (BioTek, Winooski, VT).

Scanning Electron Microscopy. SEM measurements were performed over glass coverslips treated with acid wash in 1 M HCl for 4 h at 55 °C, agitated occasionally, followed by stringent cleaning with water and 100% ethanol. Coverslips were subsequently incubated in 0.1% poly-L-lysine to improve surface adhesion. Following incubation of Aβ conditions at 37 °C for 2 weeks, sample aliquots were deposited over the coverslips and fixed with 2.5% glutaraldehyde for 1 h and then washed with 50 mM PBS. The samples were dehydrated through a multistep process starting with 50%, 70%, 95%, and 100% ethanol followed by critical point drying with liquid CO_2 and coated lightly with gold−palladium. SEM measurements were performed using a Hitachi S530 scanning electron microscope with an acceleration voltage of 20 kV and working distance of 5.0 mm.

Cell Culture, Differentiation, and Treatment. The human SH-SY5Y neuronal cell line (American Type Culture Collection, Manassas, VA) was maintained in Dulbecco's modified Eagle's medium (DMEM) supplemented with 10% fetal bovine serum (FBS). Cultures were maintained at 37 °C in a humidified 5% CO_2 atmosphere. After plating at a cell density of 4.4×10^4 cells/cm^2 and allowing for cell adhesion for 24 h, neuronal differentiation was induced by treatment with 10 μM of *all-trans*-retinoic acid at 37 °C for 72 h under serum-free condition.

Immunofluorescence and Antibodies. Differentiated human neuronal cells treated with TAE-1 or TAE-2 for 24 h were fixed with 4% paraformaldehyde in phosphate buffered saline (PBS; 137 mM NaCl, 2.7 mM KCl, 10 mM Na_2HPO_4, 2 mM KH_2PO4, pH 7.4) at room temperature for 30 min. Cells were then permeabilized with 0.1% Triton X-100 in PBS containing 100 mM glycine for 30 min, washed, and blocked with 5% fetal bovine serum (FBS) in PBS overnight. Incubation with primary antibodies was performed in 1% FBS in PBS overnight. Cells were then washed and incubated with fluorescently labeled secondary antibodies, before mounting and imaging by structural illumination using an AxioCam HRm camera with an ApoTome module on an AxioVert 200 M microscope (Carl Zeiss). Primary antibodies against α-tubulin (T9026, Sigma Aldrich), Synaptophysin (RM9111, Thermo Scientific), MAP2 (ab5392, Abcam), and βIII-tubulin (T8660, Sigma-Aldrich) were employed. Donkey anti-mouse, donkey anti-rabbit, and donkey anti-chicken Dylight secondary antibodies were purchased from Jackson ImmunoResearch Laboratories and were used at recommended dilutions.

Amperometric Quantification of Acetylcholinesterase (AChE) Activity. Purified human erythrocyte AChE was reconstituted in 20 mM Tris buffer pH 7.0, 100 mM NaCl and prepared to a working concentration of 0.1875 U/mL in 50 mM PBS, 100 mM NaCl pH 7.4. AChE was preincubated individually with either TAE-1 or TAE-2 at various concentrations for 30 min at room temperature. The enzymatic reaction was initiated by the addition of acetylthiocholine iodide (ATCh) diluted to a final concentration of 550 μM. The solution was mixed and then incubated for 10 min at room temperature, during which ATCh was hydrolyzed releasing TCh. Measurements were conducted on screen-printed electrodes (Bio Device Technology Ltd.) consisting of a gold working electrode, carbon counter electrode, and Ag/AgCl reference electrode. Following incubation, a 12 μL aliquot was deposited uniformly over the gold working electrode surface (geometric area: 2.64 mm^2). The screen-printed electrode was connected to a μAutolab-III electrochemical analysis system (Eco Chemie, Kanaalweg, The Netherlands), which was used to oxidize the TCh in solution by differential pulse voltammetry (50 mV modulation amplitude, 5 mV step potential, 50 ms modulation time, 10 s equilibration time, potential range of −0.1 to 0.9 V). AChE inhibition was determined from the anodic peak current generated by the oxidation of TCh at approximately 0.3 V (vs Ag/AgCl) of *sym*-triazine inhibited samples versus the uninhibited control. After each measurement, screen-printed electrodes were disposed of, thereby preventing contamination by electrode material from previous measurements.[24,25] Electrochemical characterization of AChE activity was further validated by Ellman's colorimetric assay.

Colorimetric Assay for the Determination of AChE Activity. The influence of *sym*-triazine compounds on the hydrolytic activity of purified human erythrocyte AChE was determined using Ellman's method adapted from Rampa and co-workers.[27,28,31] Enzyme assay solutions were prepared in a microplate well containing AChE (0.1875 U/mL) and DTNB (340 μM) in 50 mM PBS pH 7.4. The enzyme reaction was initiated by the addition of ATCh (550 μM). Pilot studies were performed to calibrate the activity of AChE expressing cytosol of differentiated human neuronal cells to that of human erythrocyte AChE, and the assay was repeated for TAE-1, TAE-2, and Donepezil. Cells were treated with TAE-1, TAE-2, or Donepezil at concentrations as specified for 24 h before assay. Optical density at 410 nm was measured in 15 s intervals for a period of 5 min using a Synergy HT Multimode Microplate reader. The initial reaction rate ($OD_{410\ nm}$/min) was determined from linear regression analysis of the absorbance time curves (n = 3). The rate of the uninhibited enzyme hydrolysis (V_o) was calibrated to 0.100 $OD_{410\ nm}$/min ± 0.030. Reaction rate was then measured in the presence of inhibitors (V_i) at various concentrations. AChE activity was determined by the expression % AChE activity = $(V_i/V_o) \times 100$. For each inhibitor, the enzyme activity was plotted as a function of the logged concentration. Nonlinear regression of inhibition plots were performed to determine the IC_{50} concentration.[28,31]

AUTHOR INFORMATION

Corresponding Author

*E-mail: kagan.kerman@utoronto.ca. Tel: +1 416 287 7249. Fax: +1 416 287 7279.

Author Contributions

A.J.V., A.M.C., I.R.B., and K.K. designed the experiments and wrote the manuscript. D.D. and S.M. synthesized the sym-triazine inhibitors. A.J.V. performed ThT fluorescence analysis and electron microscopy studies of $A\beta_{1-42}$, as well as the electrochemical and optical determination of AChE activity. A.M.C., D.W.T., and H.V.S.G. prepared differentiated cell cultures, cytosol extraction and fluorescence microscopy.

Funding

This research was carried out with the financial support of NSERC Discovery Grants to K.K. and I.R.B., a Biomedical Young Investigator Award from the Alzheimer Society of Canada to K.K., and a Canada Research Chair (Tier I) in Neuroscience to I.R.B.

Notes

The authors declare no competing financial interest.

■ ABBREVIATIONS

acetylcholinesterase, AChE; acetylthiocholine iodide, ATCh; thiocholine, TCh; thioflavin T, ThT

■ REFERENCES

(1) Selkoe, D. J. (2001) Alzheimer's disease results from the cerebral accumulation and cytotoxicity of amyloid beta-protein. *J. Alzheimer's Dis. 3*, 75−81.

(2) da Silva, G. F. Z., and Ming, L. J. (2007) Metallo-ROS in Alzheimer's disease: Oxidation of neurotransmitters by Cu-II-beta-amyloid and neuropathology of the disease. *Angew. Chem., Int. Ed. 46*, 3337−3341.

(3) Qin, L. Y., Liu, Y. X., Cooper, C., Liu, B., Wilson, B., and Hong, J. S. (2002) Microglia enhance beta-amyloid peptide-induced toxicity in cortical and mesencephalic neurons by producing reactive oxygen species. *J. Neurochem. 83*, 973−983.

(4) Scheidt, H. A., Morgado, I., Rothemund, S., Huster, D., and Fäendrich, M. (2011) Solid-state NMR spectroscopic investigation of A beta protofibrils: Implication of a beta-sheet remodeling upon maturation into terminal amyloid fibrils. *Angew. Chem., Int. Ed. 50*, 2837−2840.

(5) Walsh, D. M., and Selkoe, D. J. (2007) A beta oligomers - A decade of discovery. *J. Neurochem. 101*, 1172−1184.

(6) Nakagami, Y., Nishimura, S., Murasugi, T., Kubo, T., Kaneko, I., Meguro, M., Marumoto, S., Kogen, H., Koyama, K., and Oda, T. (2002) A novel compound RS-0466 reverses beta-amyloid-induced cytotoxicity through the Akt signaling pathway in vitro. *Eur. J. Pharmacol. 457*, 11−17.

(7) Kim, W., Kim, Y., Min, J., Kim, D. J., Chang, Y. T., and Hecht, M. H. (2006) A high-throughput screen for compounds that inhibit aggregation of the Alzheimer's peptide. *ACS Chem. Biol. 1*, 461−469.

(8) Schliebs, R., and Arendt, T. (2006) The significance of the cholinergic system in the brain during aging and in Alzheimer's disease. *J. Neural. Transm. 113*, 1625−1644.

(9) Ibach, B., and Haen, E. (2004) Acetylcholinesterase inhibition in Alzheimer's disease. *Curr. Pharm. Des. 10*, 231−251.

(10) Piazzi, L., Rampa, A., Bisi, A., Gobbi, S., Belluti, F., Cavalli, A., Bartolini, M., Andrisano, V., Valenti, P., and Recanatini, M. (2003) 3-(4-{ benzyl(methyl)amino methyl}-phenyl)-6,7-dimethoxy-2H-2-chromenone (AP2238) inhibits both acetylcholinesterase and acetylcholinesterase-induced beta-amyloid aggregation: A dual function lead for Alzheimer's disease therapy. *J. Med. Chem. 46*, 2279−2282.

(11) Cavalli, A., Bolognesi, M. L., Minarini, A., Rosini, M., Tumiatti, V., Recanatini, M., and Melchiorre, C. (2008) Multi-target-directed ligands to combat neurodegenerative diseases. *J. Med. Chem. 51*, 347−372.

(12) Huang, Y. D., and Mucke, L. (2012) Alzheimer mechanisms and therapeutic strategies. *Cell 148*, 1204−1222.

(13) Cavalli, A., Bolognesi, M. L., Capsoni, S., Andrisano, V., Bartolini, M., Margotti, E., Cattaneo, A., Recanatini, M., and Melchiorre, C. (2007) A small molecule targeting the multifactorial nature of Alzheimer's disease. *Angew. Chem., Int. Ed. 46*, 3689−3692.

(14) Dantoine, T., Auriacombe, S., Sarazin, M., Becker, H., Pere, J. J., and Bourdeix, I. (2006) Rivastigmine monotherapy and combination therapy with memantine in patients with moderately severe Alzheimer's disease who failed to benefit from previous cholinesterase inhibitor treatment. *Int. J. Clin. Pract. 60*, 110−118.

(15) Veloso, A. J., Dhar, D., Chow, A. M., Zhang, B., Tang, D. W. F., Ganesh, H. V. S., Mikhaylichenko, S., Brown, I. R., and Kerman, K. (2013) Sym-triazines for directed multitarget modulation of cholinesterases and amyloid-beta in Alzheimer's disease. *ACS Chem. Neurosci. 4*, 339−349.

(16) Pallitto, M. M., Ghanta, J., Heinzelman, P., Kiessling, L. L., and Murphy, R. M. (1999) Recognition sequence design for peptidyl modulators of beta-amyloid aggregation and toxicity. *Biochemistry 38*, 3570−3578.

(17) Ehrnhoefer, D. E., Bieschke, J., Boeddrich, A., Herbst, M., Masino, L., Lurz, R., Engemann, S., Pastore, A., and Wanker, E. E. (2008) EGCG redirects amyloidogenic polypeptides into unstructured, off-pathway oligomers. *Nat. Struct. Mol. Biol. 15*, 558−566.

(18) Bieschke, J., Russ, J., Friedrich, R. P., Ehrnhoefer, D. E., Wobst, H., Neugebauer, K., and Wanker, E. E. (2010) EGCG remodels mature alpha-synuclein and amyloid-beta fibrils and reduces cellular toxicity. *Proc. Natl. Acad. Sci. U.S.A. 107*, 7710−7715.

(19) Okabe, S., Miwa, A., and Okado, H. (2001) Spine formation and correlated assembly of presynaptic and postsynaptic molecules. *J. Neurosci. 21*, 6105−6114.

(20) Brewer, G. J., Boehler, M. D., Pearson, R. A., DeMaris, A. A., Ide, A. N., and Wheeler, B. C. (2009) Neuron network activity scales exponentially with synapse density. *J. Neural Eng. 6*, 014001.

(21) Dinsmore, J. H., and Solomon, F. (1991) Inhibition of MAP2 expression affects both morphological and cell-division phenotypes of neuronal differentiation. *Cell 64*, 817−826.

(22) Fraichard, A., Chassande, O., Bilbaut, G., Dehay, C., Savatier, P., and Samarut, J. (1995) In-vitro differentiation of embryonic stem-cells into glial-cells and functional-neurons. *J. Cell Sci. 108*, 3181−3188.

(23) Abrous, D. N., Koehl, M., and Le Moal, M. (2005) Adult neurogenesis: From precursors to network and physiology. *Physiol. Rev. 85*, 523−569.

(24) Dounin, V., Veloso, A. J., Schulze, H., Bachmann, T. T., and Kerman, K. (2010) Disposable electrochemical printed gold chips for the analysis of acetylcholinesterase inhibition. *Anal. Chim. Acta 669*, 63−67.

(25) Somji, M., Dounin, V., Muench, S. B., Schulze, H., Bachmann, T. T., and Kerman, K. (2012) Electroanalysis of amino acid substitutions in bioengineered acetylcholinesterase. *Bioelectrochemistry 88*, 110−113.

(26) Chow, A. M., and Brown, I. R. (2007) Induction of heat shock proteins in differentiated human and rodent neurons by celastrol. *Cell Stress Chaperones 12*, 237−244.

(27) Ellman, G. L., Courtney, K. D., Andres, V., and Featherstone, R. M. (1961) A new and rapid colorimetric determination of acetylcholinesterase activity. *Biochem. Pharmacol. 7*, 88.

(28) Rizzo, S., Bartolini, M., Ceccarini, L., Piazzi, L., Gobbi, S., Cavalli, A., Recanatini, M., Andrisano, V., and Rampa, A. (2010) Targeting Alzheimer's disease: Novel indanone hybrids bearing a pharmacophoric fragment of AP2238. *Bioorg. Med. Chem. 18*, 1749−1760.

(29) Hansen, R. A., Gartlehner, G., Webb, A. P., Morgan, L. C., Moore, C. G., and Jonas, D. E. (2008) Efficacy and safety of donepezil, galantamine, and rivastigmine for the treatment of Alzheimer's disease: A systematic review and meta-analysis. *Clin. Interventions Aging 3*, 211−225.

(30) Das, J. R., and Tizabi, Y. (2009) Additive protective effects of Donepezil and nicotine against salsolinol-induced cytotoxicity in SH-SY5Y cells. *Neurotoxic. Res. 16*, 194−204.

(31) Belluti, F., Piazzi, L., Bisi, A., Gobbi, S., Bartolini, M., Cavalli, A., Valenti, P., and Rampa, A. (2009) Design, synthesis, and evaluation of benzophenone derivatives as novel acetylcholinesterase inhibitors. *Eur. J. Med. Chem. 44*, 1341−1348.